LETTERS

Global and local fMRI signals driven by neurons defined optogenetically by type and wiring

Jin Hyung Lee[1,2]*, Remy Durand[2]*, Viviana Gradinaru[2], Feng Zhang[2], Inbal Goshen[2], Dae-Shik Kim[3,4], Lief E. Fenno[2], Charu Ramakrishnan[2] & Karl Deisseroth[2,5,6,7]

Despite a rapidly-growing scientific and clinical brain imaging literature based on functional magnetic resonance imaging (fMRI) using blood oxygenation level-dependent (BOLD)[1] signals, it remains controversial whether BOLD signals in a particular region can be caused by activation of local excitatory neurons[2]. This difficult question is central to the interpretation and utility of BOLD, with major significance for fMRI studies in basic research and clinical applications[3]. Using a novel integrated technology unifying optogenetic[4–13] control of inputs with high-field fMRI signal readouts, we show here that specific stimulation of local CaMKIIα-expressing excitatory neurons, either in the neocortex or thalamus, elicits positive BOLD signals at the stimulus location with classical kinetics. We also show that optogenetic fMRI (ofMRI) allows visualization of the causal effects of specific cell types defined not only by genetic identity and cell body location, but also by axonal projection target. Finally, we show that ofMRI within the living and intact mammalian brain reveals BOLD signals in downstream targets distant from the stimulus, indicating that this approach can be used to map the global effects of controlling a local cell population. In this respect, unlike both conventional fMRI studies based on correlations[14] and fMRI with electrical stimulation that will also directly drive afferent and nearby axons, this ofMRI approach provides causal information about the global circuits recruited by defined local neuronal activity patterns. Together these findings provide an empirical foundation for the widely-used fMRI BOLD signal, and the features of ofMRI define a potent tool that may be suitable for functional circuit analysis as well as global phenotyping of dysfunctional circuitry.

Blood oxygenation level-dependent functional magnetic resonance imaging (BOLD fMRI)[1] is a widely used technology for non-invasive whole brain imaging. BOLD signals reflect complex and incompletely understood changes in cerebral blood flow (CBF), cerebral blood volume (CBV), and cerebral metabolic rate of oxygen consumption ($CMRO_2$) following neuronal activity[2,15]. Candidate circuit elements for triggering various kinds of BOLD signals include excitatory neurons, mixed neuronal populations, astroglia, and axonal tracts or fibres of passage[16,17]. Importantly, it is not clear which kinds of activity are capable of triggering BOLD responses, placing limitations on interpretation for both clinical and scientific applications. For example, it is sometimes assumed that positive BOLD signals can be triggered by increased activity of local excitatory neurons, but this remains to be shown empirically, a challenge that seriously confounds fMRI interpretation[18,19]. Moreover, the use of MRI-compatible electrodes for local stimulation, although of pioneering significance, will nevertheless drive all local excitatory, inhibitory, and modulatory cell types, as well as antidromically drive non-local cells that happen to have axons within the stimulated region, thereby confounding functional circuit mapping using BOLD. We sought to address these challenges by integrating high-field fMRI output with optogenetic stimulation[4–13], in which single-component microbial light-activated transmembrane conductance regulators are introduced into specifically targeted cell types and circuit elements[7,8] using cell type-specific promoters to allow millisecond-scale targeted activity modulation *in vivo*[9–11].

In adult rats, the primary motor cortex (M1) was injected with the adeno-associated viral vector AAV5-CaMKIIα::ChR2(H134R)-EYFP to drive expression of a channelrhodopsin (ChR2) specifically in Ca^{2+}/calmodulin-dependent protein kinase II α (CaMKIIα)-expressing principal cortical neurons, but not in GABAergic or glial cells[7,9–12]; here the cortical virus injection site was also used as the optical stimulation site for BOLD and electrophysiological functional studies (Fig. 1a). To minimize susceptibility artefact during MRI scanning, the implanted cannula, optical fibre and accessories were custom-fabricated from magnetic resonance-compatible materials. Confocal imaging (Fig. 1b) and optrode recording (simultaneous optical stimulation and electrical recording) under 1.3–1.5% isoflurane anaesthesia[20] (Fig. 1c) were conducted to validate the expression and functionality, respectively, of the ChR2–EYFP (enhanced yellow fluorescent protein) fusion under these conditions. In line with previous optogenetic studies[11], 473 nm light pulses at 20 Hz (15 ms pulse width) delivered through the optical fibre were found to drive local neuronal firing reliably *in vivo* (Fig. 1c).

To assess fMRI signals, we acquired 0.5 mm coronal slices centred on M1, >10 days after virus injection (Fig. 1d). Intubated animals were placed on a custom-designed MRI-compatible cradle with a stereotaxic frame and ventilated with 1.3–1.5% isoflurane. A 3.5 cm-diameter custom-designed transmit/receive single-loop surface coil was apposed to the cranium and a long 300-μm diameter optical fibre inserted through the implanted cannula; in this configuration, the cradle with the animal was placed into the iso-centre of the magnet while the laser diode itself was maintained outside the 5 Gauss perimeter. To minimize systemic physiological confounds, the ventilation volume, frequency, end-tidal CO_2 and rectal temperature levels were carefully maintained at narrow levels known to produce most robust and reproducible BOLD signals in anaesthetized animals (3.0–3.5 cm^3 per stroke, 50–60 strokes per min, 3.5%, 34–38 °C)[20]. fMRI scans were performed at 7.0 Tesla (T) field strength using conventional gradient-echo (GRE)-BOLD fMRI and pass-band balanced steady-state free

[1]Department of Electrical Engineering, Psychiatry and Biobehavioral Sciences, Bioengineering, and Radiology, University of California, Los Angeles, California 90095, USA. [2]Department of Bioengineering, Stanford University, Stanford, California 94305, USA. [3]Department of Electrical Engineering, Korea Advanced Institute of Science and Technology (KAIST), Daejeon 305-701, Republic of Korea. [4]Department of Anatomy and Neurobiology, Boston University School of Medicine, Boston, Massachusetts 02118, USA. [5]Howard Hughes Medical Institute, Stanford University, Stanford, California 94305, USA. [6]CNC Program, Stanford University, Stanford, California 94305, USA. [7]Department of Psychiatry and Behavioral Sciences, Stanford, California 94305, USA.
*These authors contributed equally to this work.

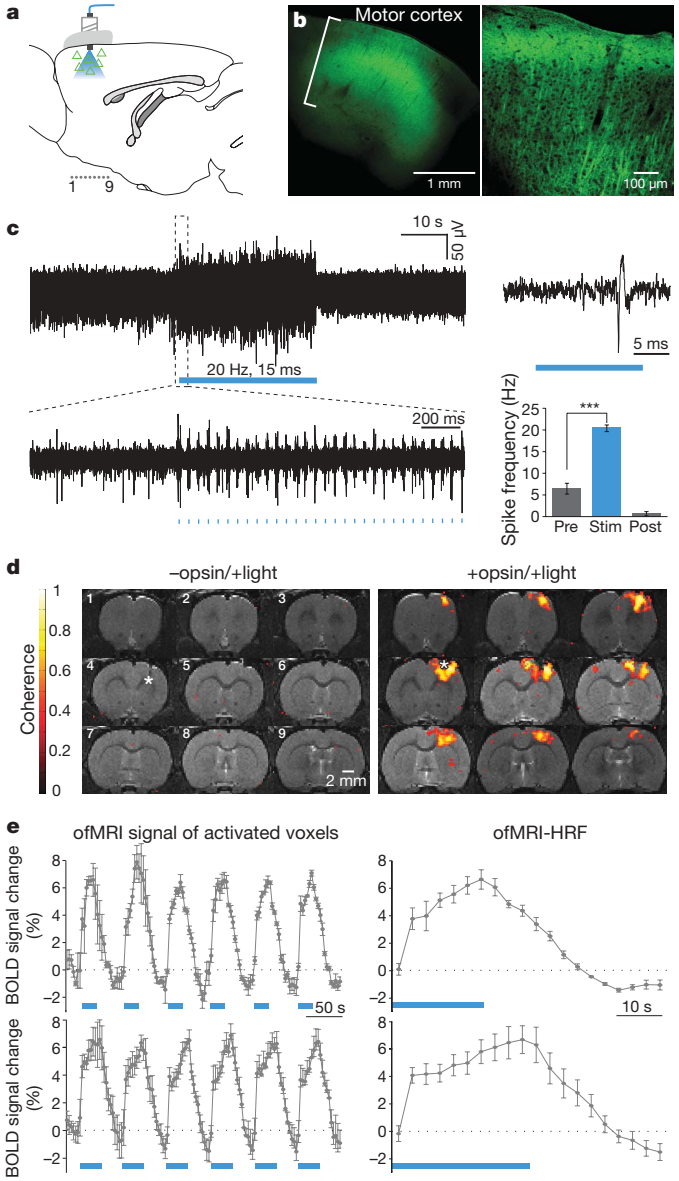

Figure 1 | ofMRI: optogenetic excitation of CaMKIIα neocortical cells drives local positive BOLD. **a**, Transduced cells (triangles), light and location (1…9) of coronal slices. **b**, Confocal images of ChR2–EYFP expression in M1 (left); higher magnification (right). **c**, Optrode recordings during 473 nm optical stimulation (20 Hz/15 ms pulse width; blue); spiking is significantly elevated (error bar indicates ± s.d., two-sample *t*-test; *** indicates $P < 0.001$; $n = 3$). Pre, pre-stimulation; Stim, during stimulation; Post, post-stimulation. **d**, BOLD activation observed with AAV5-CaMKIIα::ChR2-EYFP but not with saline injection ($P < 0.001$; asterisk, optical stimulation). **e**, Left, ofMRI haemodynamic response (averaged across activated voxels in motor cortex) during 20 s (top) and 30 s (bottom) optical stimuli. Right, mean over stimulus repetitions; baseline, mean pre-stimulation signal. Top panels, $n = 3$; bottom panels, $n = 8$.

precession (b-SSFP)-fMRI[21,22] (Supplementary Material). Both pulse sequences were designed to have $3.5 \times 3.5\ cm^2$ in-plane field of view (FOV), $0.5 \times 0.5 \times 0.5\ mm^3$ spatial resolution and 3 s temporal resolution. GRE-BOLD fMRI was designed to be a two-dimensional, multi-slice, gradient-echo sequence with four-interleave spiral readout[23]; 750 ms repetition time (T_R) and 12 ms echo time (T_E) resulting in 23 slices covering 1.15 cm slice direction volume. This specific design allowed large-volume mapping of the brain during optogenetic control with high temporal resolution.

Light pulses at 20 Hz (473 nm, 15 ms pulse width) were delivered to targeted CaMKIIα-expressing principal neurons, and in response, robust optically-evoked BOLD signals were observed in cortical grey matter at the virus injection and optical stimulation site, whereas in control animals (injected with saline instead of opsin-AAV) no detectable BOLD signal could be elicited (Fig. 1). Stimulus-synchronized BOLD haemodynamic responses from activated M1 voxels are displayed in Fig. 1d, and mean optogenetic fMRI haemodynamic response functions (ofMRI-HRF) in Fig. 1e. Evoked BOLD was dominated by positive signals while driving these excitatory CaMKIIα-positive cells; in contrast, optically driving inhibitory parvalbumin-positive cells[10], which may have unique connectivity with local neuronal circuitry or vasculature, additionally gave rise to a zone of negative BOLD, consistent with the GABAergic phenotype, surrounding the local positive BOLD signal (Supplementary Fig. 4). Strikingly, the BOLD dynamics observed by optically driving the defined CaMKIIα principal cell population embedded within the mixed M1 cell population precisely matched the dynamics of conventional stimulus-evoked BOLD-fMRI[24,25]. In particular, the ofMRI-HRF signal onset occurred after 3 s but within 6 s of stimulus onset; likewise offset was reflected by a drop in BOLD signal contrast beginning within 6 s and returning to baseline in ~20 s after optical stimulation (Fig. 1e; upper panels: $n = 3$, lower panels: $n = 8$). Finally, the pronounced post-stimulus undershoot observed during systemic somatosensory stimulation in humans[26] and animals[24] was preserved in ofMRI-HRFs as well (Fig. 1e). All of these dynamic properties derived from driving a defined, specific (Methods; Supplementary Fig. 1a) cell population correspond closely to previous measurements on conventional sensory-evoked BOLD.

To study macrocircuit properties of the brain using optogenetic fMRI, it will be important to assess feasibility of monitoring long-range activity in synaptically connected brain areas. MRI-compatible electrodes for local stimulation represent a major advance but in addition to driving all local excitatory, inhibitory and modulatory cell types, will also antidromically drive non-local cells that happen to have axons within the stimulated region, posing a challenge for functional mapping using BOLD. We therefore used high-resolution fMRI slices capturing thalamic nuclei (coronal slices shown in Fig. 2a) to monitor downstream responses during optical stimulation of M1 cortical neurons. Figure 2b illustrates the observed specific ChR2 expression in cortico-thalamic axonal projection fibres whereas thalamic cell bodies showed no ChR2 expression, as expected from the cortical injection protocol (Supplementary Fig. 5). Local optical stimulation was then delivered to the cortex during fMRI, to determine if unidirectionally triggered BOLD responses could be observed and measured (this method eliminates the antidromic drive confound from which electrical stimulation suffers, thereby allowing true global causal connectivity mapping). Figure 2c and d summarize the thalamic ofMRI-HRFs; robust thalamic BOLD signals in response to M1 stimulation were observed, but with properties quite distinct from the intracortical CaMKIIα+ response described above. A markedly reduced initial rise and slope for onset kinetics of positive-BOLD downstream thalamic recruitment was observed (Fig. 2d, black traces; local cortical BOLD signals shown for comparison, grey traces; cortical BOLD activation is shown in Fig. 1).

Given the unusual kinetics, we sought to determine if this delayed thalamic BOLD response would be discrepant with local thalamic electrical activity, assessed with simultaneous optrode stimulating/recording in motor cortex and electrode recoding in thalamus (Fig. 2e). However, a strikingly similar pattern was observed with direct recording in thalamus, including a commensurate delay in spike-rate increase for thalamic neurons compared to cortical neurons during cortical optogenetic drive (Fig. 2f), further supporting the tight correspondence between positive BOLD and local neuronal excitation[2,27,28]. Additional characterization showed that after this ~5 s delay presumably related to network properties, successfully evoked spikes recorded in the thalamus reliably followed cortical spikes by several milliseconds, as expected (Fig. 2g). Summary data on mean spike rates is presented in Fig. 2h, and on spike rate dynamics in Fig. 2i; further details on the pass-band bSSFP-fMRI[21,22] method we

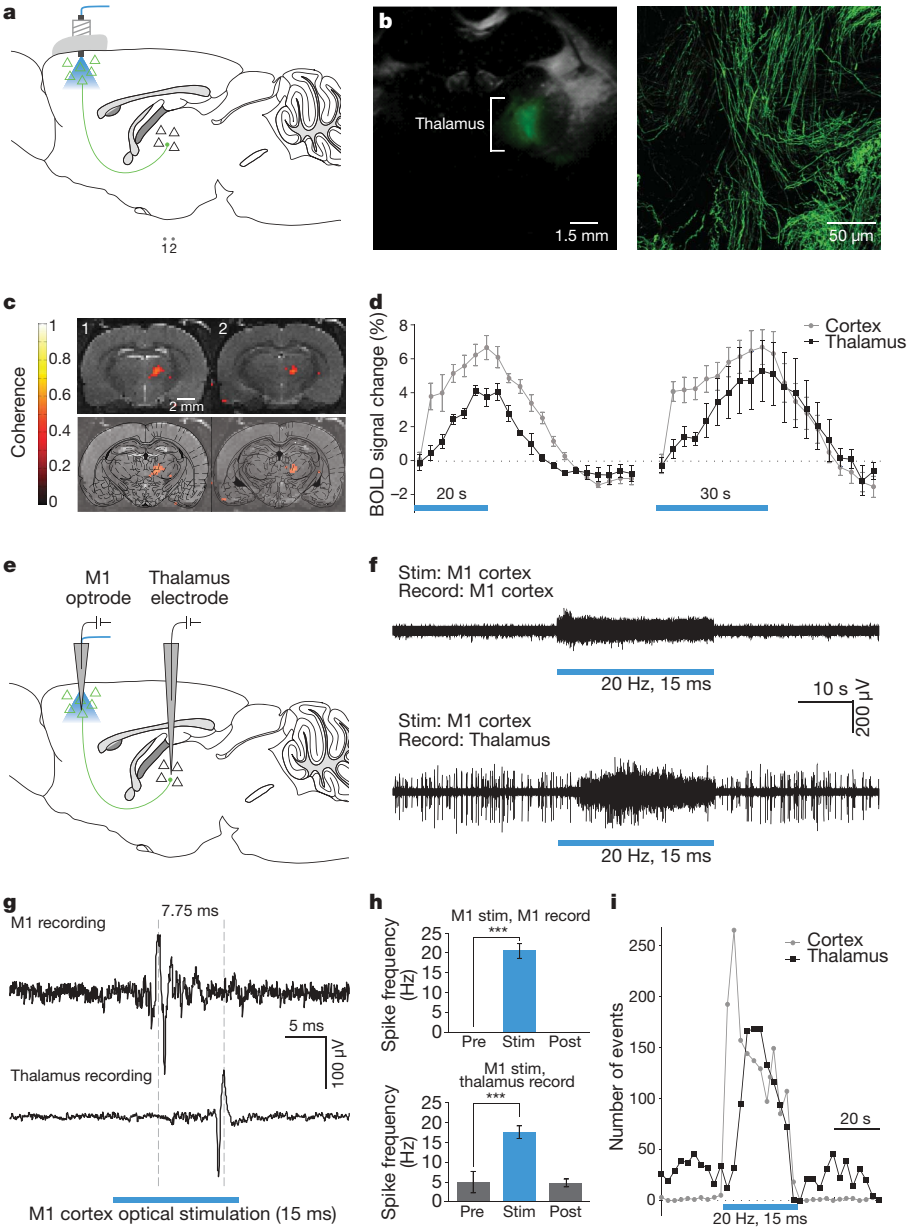

Figure 2 | Nonlocal mapping of the causal role of cells defined by location and genetic identity. **a**, AAV5-CaMKIIα::ChR2-EYFP injection and optical stimulation in M1. Slices in **c**: '1' and '2'. **b**, Fluorescence/bright-field: ChR2–EYFP in thalamus (left); confocal image shows expression limited to axons. **c**, Thalamic ofMRI during M1 optical stimulation (top); superimposed on the Paxinos atlas (bottom). **d**, ofMRI-HRF summary. **e**, M1 optrode and thalamic electrode. **f**, Thalamic spiking follows M1 optical stimulation; delay consistent with BOLD. **g**, Typical M1 and thalamus spikes with M1 optical excitation. **h**, M1 and thalamus spiking summary (error bar indicates ± s.d., two-sample *t*-test; *** indicates $P < 0.001$; $n = 5$). **i**, Spike-frequency time histograms.

developed for small animal imaging with more robust whole-brain mapping capability than traditional BOLD are presented in the Supplementary Material (Supplementary Fig. 3).

Because true functional outputs of genetically defined neurons in a brain region can be globally mapped with ofMRI (Fig. 2), it is conceivable that additional levels of specificity could also be achieved. For example, M1 excitatory pyramidal neurons form a genetically and anatomically defined class of cell, but within this class are cells that each project to different areas of the brain or spinal cord and therefore have fundamentally distinct roles. Genetic tools may not advance far enough to separate all of these different cell classes, pointing to the need for other promoter-independent targeting methods[13]. But ofMRI raises the current possibility of globally mapping the causal roles of these cells, accessing them by means of connection topology—that is, by the conformation of their functional projection patterns in the brain. We therefore sought to test this possibility by selectively driving the M1 CaMKIIα-expressing cells that project to the thalamus.

An optical fibre was stereotactically placed in the thalamus of animals that had received M1 cortical viral injections (Fig. 3a); post hoc validation (Fig. 3b) confirmed ChR2 expression in cortical neurons and in cortico-thalamic projection fibres. ChR2 readily triggers spikes in illuminated photosensitive axons that both drive local synaptic output and back-propagate throughout the axon to the soma of the stimulated cell; note that unlike the case with electrical stimulation, specificity is maintained for driving the targeted (photosensitive) axons, and therefore this configuration in principle allows ofMRI mapping during selective control of the M1 cortical cells that project to the thalamus. Indeed, robust BOLD signals were observed both locally in the thalamus (Fig. 3c, coronal slices 7–12) and also in M1 (Fig. 3d, coronal slices 1–6), consistent with the anticipated recruitment of the topologically targeted cells both locally and distally. These data demonstrate that ChR2-expressing axonal fibre stimulation alone is sufficient to elicit BOLD responses in remote areas, and illustrate the feasibility for *in vivo* mapping of the global impact of cells defined not only by anatomical location and genetic identity, but also by connection topology.

We further explored the global mapping capabilities of ofMRI. It has been suggested that thalamic projections to the motor cortex may be more likely than those to the sensory cortex, to involve both ipsilateral and contralateral pathways, because in many cases motor control and planning must involve bilateral coordination[29]. This principle is challenging to assess at the functional level, because electrode-based stimulation will drive antidromic as well as orthodromic projections,

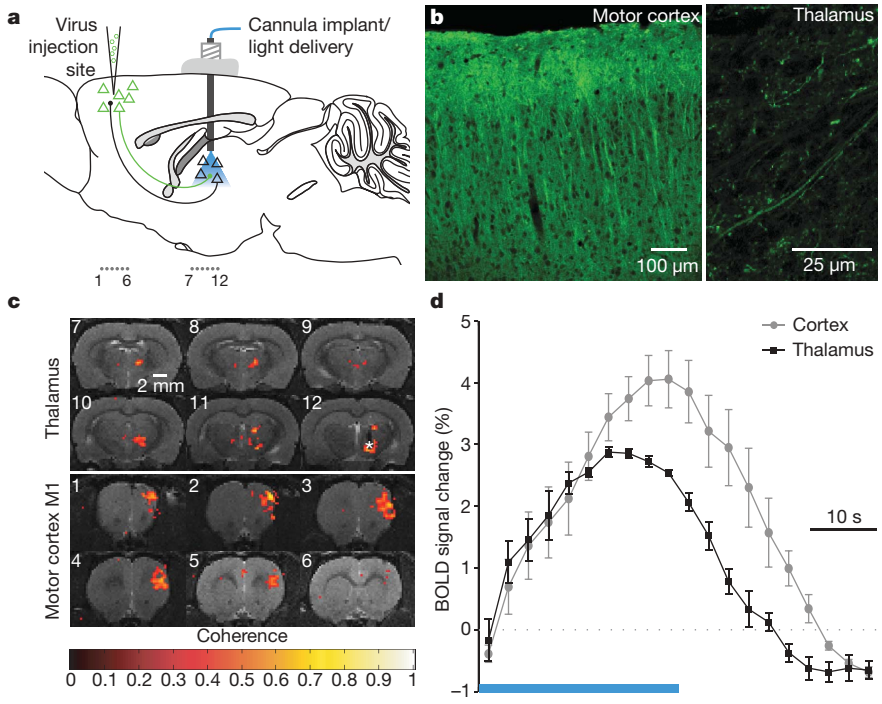

Figure 3 | Control of cells defined by location, genetic identity and wiring during ofMRI. **a**, M1 injection of AAV5-CaMKIIα::ChR2-EYFP and optical stimulation of the thalamus. Coronal slices shown in **c** marked as '1…6' and '7…12'. **b**, ChR2 expression pattern confirming expression in cortical neurons (left) and cortico-thalamic projections (right; see also Supplementary Fig. 5). **c**, BOLD ofMRI data obtained in thalamus (above) and cortex (below). **d**, ofMRI-HRF for cortical (grey) and thalamic (black) BOLD signals elicited by optical stimulation of cortico-thalamic fibres in thalamus. Both ofMRI-HRFs ramp slowly by comparison with intracortical results in Fig. 1.

and hence may mistakenly report robust cortico-thalamic rather than thalamocortical projections. We therefore sought to globally map functional connectivity arising from the initial drive of anterior or posterior thalamic nucleus projections, using ofMRI. After injecting CaMKIIα::ChR2 into the thalamus (Fig. 4), we found that optical stimulation of posterior thalamic nuclei resulted in a strong BOLD response, both at the site of stimulation as expected and in the posterior ipsilateral somatosensory cortex (S2) (Fig. 4a–d). Optically stimulating excitatory cell bodies and fibres in the more anterior thalamic nuclei resulted in BOLD response at the site of stimulation and also significant ipsilateral and contralateral cortical BOLD responses (Fig. 4e, f), consistent with the proposed bilaterality of anterior thalamocortical nuclei involvement in motor control and coordination[30].

Together, these results illustrate the power of optogenetic fMRI in shedding light on the controversial identification of positive BOLD signals with increased local neuronal excitation, providing an empirical underpinning for fMRI BOLD. We also find that the properties of

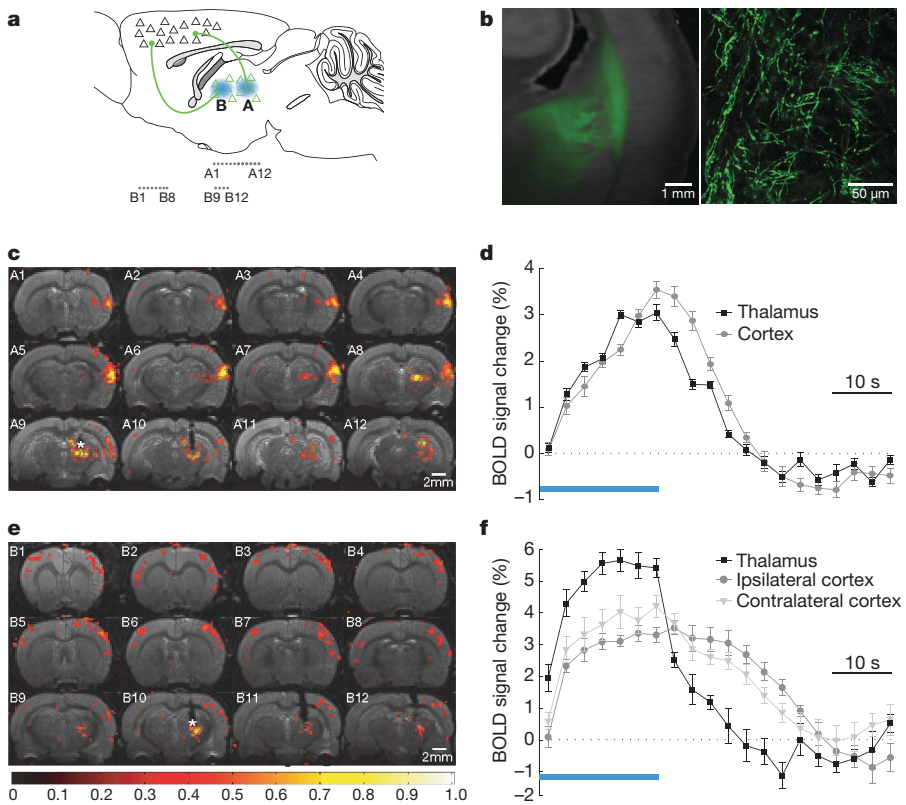

Figure 4 | Recruitment of bilateral cortices by the anterior thalamus. **a**, Thalamic injection of AAV5-CaMKIIα::ChR2-EYFP and posterior/ anterior optical stimulation. Coronal slices marked 'A1…A12' and 'B1…B12'. **b**, Fluorescence overlaid onto bright-field (left) and confocal image (right) illustrating transduction in the thalamus (left) and cortical projections in the internal and external capsule (right). **c**, Posterior thalamus stimulation-evoked ofMRI signal in the ipsilateral thalamus and somatosensory cortex. **d**, ofMRI-HRFs. Excited volumes: 5.5 ± 1.3 mm^3 (thalamus); 8.6 ± 2.5 mm^3 (somatosensory cortex) ($n = 3$). **e**, Anterior thalamus stimulation-evoked ofMRI signal in the ipsilateral thalamus and bilateral motor cortex. **f**, ofMRI-HRFs. Excited volumes: 1.5 mm^3 (thalamus); 10.1 mm^3 (ipsilateral cortex); 3.7 mm^3 (contralateral cortex).

integrated optogenetics and BOLD-fMRI (ofMRI) allow for global mapping of the causal connectivity of defined neurons in specific brain regions, fundamentally extending the capabilities of pharmacological or electrode-based methods (of course, contributions from additional cells and processes downstream of the defined optically-triggered population are expected and indeed represent an important aspect of this approach; it is, however, important to note that absence of a BOLD signal does not prove the absence of connectivity). Finally, we demonstrate that ofMRI allows causal connectivity mapping of cells defined not only genetically but also by circuit topology, or the conformation of their connections *in vivo*. Together, the ofMRI methods and findings reported here provide tools and approaches for further probing and defining the causal generation of BOLD signals; these results may accelerate the search for global circuit-disease endophenotypes, as well as the dynamical mapping and reverse engineering of intact neural circuitry.

METHODS SUMMARY

Virus-mediated opsin expression. The pAAV-CaMKIIα-hChR2(H134R)-EYFP plasmid was designed and constructed by standard methods and packaged as AAV5. Virus was stereotaxically injected and cannulas placed at the locations where optical stimulation was planned[12]. Concentrated virus was delivered using a 10-μl syringe and 34-gauge needle; volume and flow rate ($0.1\ \mu l\ min^{-1}$) were controlled by injection pump. Maps and clones are available at http://www.optogenetics.org.

Optogenetic fMRI. Rodent subjects were connected to the optical fibre and ventilator (1.3% isoflurane), physiological monitoring systems and radio-frequency coil, and placed in the magnetic resonance-compatible stereotaxic frame. After subject placement in the scanner, blue (473 nm) light pulsed at 20 Hz (15 ms pulse width) was periodically applied through the optical fibre at 1 min intervals while repeated BOLD scans of large brain volumes[21,22] were conducted.

***In vivo* recording and analysis.** After ofMRI, simultaneous optical stimulation and electrical recording in living rodents was conducted using an optrode composed of an extracellular tungsten electrode (1 MΩ, ~125 μm) attached to an optical fibre (~200 μm) with the tip of the electrode deeper than the tip of the fibre to ensure illumination of the recorded neurons[12].

Opsin expression validation and immunohistochemistry. To validate specificity, sensitivity and spatial distribution of opsin expression, brain slices were prepared for optical microscopy and immunohistochemistry. Coronal sections (40-μm thick) were cut on a freezing microtome and stored in cryoprotectant (25% glycerol, 30% ethylene glycol, in PBS) at 4 °C until processed for immunohistochemistry. Confocal fluorescence images were acquired on a scanning laser microscope using oil immersion objectives[12].

Received 4 September 2009; accepted 26 April 2010.
Published online 16 May; corrected 10 June 2010 (see full-text HTML version for details).

1. Ogawa, S. *et al.* Intrinsic signal changes accompanying sensory stimulation: Functional brain mapping with magnetic resonance imaging. *Proc. Natl Acad. Sci. USA* **89,** 5951–5955 (1992).
2. Logothetis, N. K., Pauls, J., Augath, M., Trinath, T. & Oeltermann, A. Neurophysiological investigation of the basis of the fMRI signal. *Nature* **412,** 150–157 (2001).
3. Cohen, J. D. & Blum, K. I. Reward and decision. *Neuron* **36,** 193–198 (2002).
4. Boyden, E. S., Zhang, F., Bamberg, E., Nagel, G. & Deisseroth, K. Millisecond-timescale, genetically targeted optical control of neural activity. *Nature Neurosci.* **8,** 1263–1268 (2005).
5. Zhang, F., Wang, L. P., Boyden, E. S. & Deisseroth, K. Channelrhodopsin-2 and optical control of excitable cells. *Nature Methods* **3,** 785–792 (2006).
6. Deisseroth, K. *et al.* Next-generation optical technologies for illuminating genetically targeted brain circuits. *J. Neurosci.* **26,** 10380–10386 (2006).
7. Zhang, F. *et al.* Multimodal fast optical interrogation of neural circuitry. *Nature* **446,** 633–639 (2007).
8. Zhang, F., Aravanis, A. M., Adamantidis, A., de Lecea, L. & Deisseroth, K. Circuit-breakers: optical technologies for probing neural signals and systems. *Nature Rev. Neurosci.* **8,** 577–581 (2007).
9. Aravanis, A. M. *et al.* An optical neural interface: *in vivo* control of rodent motor cortex with integrated fiberoptic and optogenetic technology. *J. Neural Eng.* **4,** S143–S156 (2007).
10. Sohal, V. S., Zhang, F., Yizhar, O. & Deisseroth, K. Parvalbumin neurons and gamma rhythms enhance cortical circuit performance. *Nature* **459,** 698–702 (2009).
11. Gradinaru, V., Mogri, M., Thompson, K. R., Henderson, J. M. & Deisseroth, K. Optical deconstruction of parkinsonian neural circuitry. *Science* **324,** 354–359 (2009).
12. Zhang, F. *et al.* Optogenetic interrogation of neural circuits: technology for probing mammalian brain structures. *Nature Protocols* **5,** 439–456 (2010).
13. Gradinaru, V. *et al.* Molecular and cellular approaches for diversifying and extending optogenetics. *Cell* **141,** 154–165 (2010).
14. Friston, K. J. Functional and effective connectivity in neuroimaging: a synthesis. *Hum. Brain Mapp.* **2,** 56–78 (1994).
15. Uğurbil, K. *et al.* Functional mapping in the human brain using high magnetic fields. *Phil. Trans. R. Soc. Lond. B* **354,** 1195–1213 (1999).
16. Logothetis, N. K. What we can do and what we cannot do with fMRI. *Nature* **453,** 869–878 (2008).
17. Douglas, R. J. & Martin, K. A. A functional microcircuit for cat visual cortex. *J. Physiol. (Lond.)* **440,** 735–769 (1991).
18. Sirotin, Y. B. & Das, A. Anticipatory haemodynamic signals in sensory cortex not predicted by local neuronal activity. *Nature* **457,** 475–479 (2009).
19. Cauli, B. *et al.* Cortical GABA Interneurons in neurovascular coupling: relays for subcortical vasoactive pathways. *J. Neurosci.* **24,** 8940–8949 (2004).
20. Masamoto, K., Kim, T., Fukuda, M., Wang, P. & Kim, S. G. Relationship between neural, vascular, and BOLD signals in isoflurane-anesthetized rat somatosensory cortex. *Cereb. Cortex* **17,** 942–950 (2007).
21. Lee, J. H. *et al.* Full-brain coverage and high-resolution imaging capabilities of passband b-SSFP fMRI at 3T. *Magn. Reson. Med.* **59,** 1099–1110 (2008).
22. Lee, J. H., Hargreaves, B. A., Hu, B. S. & Nishimura, D. G. Fast 3D imaging using variable-density spiral trajectories with applications to limb perfusion. *Magn. Reson. Med.* **50,** 1276–1285 (2003).
23. Glover, G. H. & Lee, A. T. Motion artifacts in fMRI: comparison of 2DFT with PR and spiral scan methods. *Magn. Reson. Med.* **33,** 624–635 (1995).
24. Buxton, R. B., Wong, E. C. & Frank, L. R. Dynamics of blood flow and oxygenation changes during brain activation: the balloon model. *Magn. Reson. Med.* **39,** 855–864 (1998).
25. Boynton, G. M., Engel, S. A., Glover, G. H. & Heeger, D. J. Linear systems analysis of functional magnetic resonance imaging in human V1. *J. Neurosci.* **16,** 4207–4221 (1996).
26. Donahue, M. J. *et al.* Theoretical and experimental investigation of the VASO contrast mechanism. *Magn. Reson. Med.* **56,** 1261–1273 (2006).
27. Lauritzen, M. Reading vascular changes in brain imaging: is dendritic calcium the key? *Nature Rev. Neurosci.* **6,** 77–85 (2005).
28. Nir, Y., Dinstein, I., Malach, R. & Heeger, D. J. BOLD and spiking activity. *Nature Neurosci.* **11,** 523–524, author reply 524 (2008).
29. Alloway, K. D., Olson, M. L. & Smith, J. B. Contralateral corticothalamic projections from MI whisker cortex: potential route for modulating hemispheric interactions. *J. Comp. Neurol.* **510,** 100–116 (2008).
30. Kuramoto, E. *et al.* Two types of thalamocortical projections from the motor thalamic nuclei of the rat: a single neuron-tracing study using viral vectors. *Cereb. Cortex* **19,** 2065–2077 (2009).

Supplementary Information is linked to the online version of the paper at www.nature.com/nature.

Acknowledgements J.H.L. is supported by NIH pathway to independence grant (K99/R00) 1K99EB008738. R.D. is supported by an NSF Graduate Research Fellowship. V.G. is supported by SGF and SIGF (Stanford Graduate Fellowships). We acknowledge G. H. Glover, J. M. Pauly and D. G. Nishimura for generous support and advice, and C. Pacharinsak for assistance with rat intubation. We would also like to thank the entire Deisseroth laboratory for discussions and support, and Lee laboratory students, V. Karasev, Z. Fang and C. Jones for help with histological quantification and fMRI data analysis. K.D. is supported by the Keck, Snyder, Woo, Yu, McKnight, and Coulter Foundations, as well as by CIRM, NIMH, NIDA and the NIH Director's Pioneer Award.

Author Contributions J.H.L., F.Z., R.D., V.G. and K.D. designed the experiments. D.-S.K. provided information on the animal fMRI setup, J.H.L. developed the fMRI methods, and J.H.L. and R.D. conducted all ofMRI experiments. R.D., V.G. and F.Z. conducted animal surgery and preparation. J.H.L., L.E.F., R.D. and V.G. conducted optrode recordings. R.D., V.G. and I.G. acquired the confocal microscope images. J.H.L., R.D. and I.G. performed histology and confocal imaging for quantification. C.R. prepared the viral vectors. J.H.L., R.D., V.G., F.Z., D.-S.K. and K.D. prepared the figures and wrote the paper. K.D. supervised all aspects of the work.

Author Information Reprints and permissions information is available at www.nature.com/reprints. The authors declare no competing financial interests. Readers are welcome to comment on the online version of this article at www.nature.com/nature. Correspondence and requests for materials should be addressed to J.H.L. (ljinhy@gmail.com) and K.D. (deissero@stanford.edu).